Measurement report: Emission factors of NH_3 and NH_x for wildfires and agricultural fires in the United States

Laura Tomsche[1,2,3,+], Felix Piel[4,5,6], Tomas Mikoviny[5], Claus J. Nielsen[5], Hongyu Guo[7], Pedro Campuzano-Jost[7], Benjamin A. Nault[8], Melinda K. Schueneman[7], Jose L. Jimenez[7], Hannah Halliday[9], Glenn Diskin[2], Joshua P. DiGangi[2], John B. Nowak[2], Elizabeth B. Wiggins[1,2], Emily Gargulinski[10], Amber J. Soja[2,10], and Armin Wisthaler[4,6]

[1]Universities Space Research Association, Columbia, MD, USA
[2]NASA Langley Research Center, Hampton, VA, USA
[3]Institute of Atmospheric Physics, German Aerospace Center, Oberpfaffenhofen, Germany
[4]Department of Chemistry, University of Oslo, Oslo, Norway
[5]IONICON Analytik GmbH, Innsbruck, Austria
[6]Institut für Ionenphysik und Angewandte Physik, Universität Innsbruck, Innsbruck, Austria
[7]Department of Chemistry and Cooperative Institute for Research in Environmental Sciences (CIRES), University of Colorado, Boulder, CO, USA
[8]Center for Aerosol and Cloud Chemistry, Aerodyne Research, Inc., Billerica, MA, USA
[9]US Environmental Protection Agency, Durham, NC, USA
[10]National Institute of Aerospace, Hampton, VA, USA
[+]now at: Institute of Atmospheric Physics, Johannes-Gutenberg University Mainz, Mainz, Germany

Correspondence to: Armin Wisthaler (armin.wisthaler@kjemi.uio.no)

Abstract. During the 2019 Fire Influence on Regional to Global Environments and Air Quality (FIREX-AQ) study, the NASA DC-8 carried out *in situ* chemical measurements in smoke plumes emitted from wildfires and agricultural fires in the contiguous US. The DC-8 payload included a modified proton-transfer-reaction time-of-flight mass spectrometer (PTR-ToF-MS) for the fast measurement of gaseous ammonia (NH_3) and a high-resolution time-of-flight aerosol mass spectrometer (AMS) for the fast measurement of submicron particulate ammonium (NH_4^+). We herein report data collected in smoke plumes emitted from six wildfires in the Western US, two prescribed grassland fires in the Central US, one prescribed forest fire in the Southern US, and 66 small agricultural fires in the Southeastern US. Smoke plumes contained double to triple digit ppb levels of NH_3. In the wildfire plumes, a significant fraction of NH_3 had already been converted to NH_4^+ at the time of sampling (≥ 2 h after emission). Substantial amounts of NH_4^+ were also detected in freshly emitted smoke from corn and rice field fires. We herein present a comprehensive set of emission factors of NH_3 and NH_x, with $NH_x = NH_3 + NH_4^+$. Average NH_3 and NH_x emission factors for wildfires in the Western US were 1.86 ± 0.75 g kg^{-1} of fuel burned and 2.47 ± 0.80 g kg^{-1}, respectively. Average NH_3 and NH_x emission factors for agricultural fires in the Southeastern US were 0.89 ± 0.58 g kg^{-1} and 1.74 ± 0.92 g kg^{-1}, respectively. Our data show no clear inverse correlation between modified combustion efficiency (MCE) and NH_3 emissions. Importantly, we found that NH_3 emissions in ambient sampling were significantly higher than observed in previous laboratory experiments with similar fuel types.

1 Introduction

Ammonia (NH$_3$) is an important trace gas in the Earth's atmosphere that is mostly emitted from agriculture, traffic, the oceans and biomass burning. In the presence of acids, NH$_3$ rapidly partitions to aerosol particles, which in turn impact air quality and climate (Seinfeld and Pandis, 2016). In much of the atmosphere, NH$_3$ exhibits a major influence on particle acidity (pH), which

40 is a major controlling parameter for many important aerosol physical and chemical processes (*e.g.*, Pye et al., 2020; Nault et al., 2021). NH$_3$ is also the largest contributor to deposition of nitrogen from the atmosphere to soil and vegetation, causing surface water eutrophication, soil acidification, and ultimately biodiversity loss (*e.g.*, Bobbink and Higgs, 2014).

Fires emit NH$_3$ predominantly during smoldering combustion, which occurs at low temperatures (*e.g.*, Lobert et al., 1990; Yokelson et al., 1996, 1997; Goode et al., 1999; McMeeking et al., 2009; Burling et al., 2010; Roberts et al., 2020). NH$_3$ is

45 typically the third most abundant nitrogen compound (after N$_2$ and NO) and the most abundant reduced nitrogen compound emitted from fires (Lobert et al., 1990; Roberts et al., 2020; Lindaas et al., 2021).

An important parameter for investigating the atmospheric impact of NH$_3$ is the emission factor, EF_{NH_3}, which is the mass of NH$_3$ (in g) that is emitted per mass of fuel burned (in kg). Several literature reviews (Andreae and Merlet, 2001; Akagi et al, 2011; Andreae, 2019; Prichard et al., 2020) report EF_{NH_3} values for different types of fire fuels. A closer look at the literature

50 reveals that emissions from fuels that are typical of the United States (US) have mostly been studied in the laboratory (*e.g.,* Yokelson et al., 1996; McMeeking et al., 2009; Burling et al., 2010; Stockwell et al., 2015; Selimovic et al., 2018; Roberts et al., 2020). Previous work has shown that laboratory fires may not realistically simulate fires occurring in the real world due to different burning conditions and the lack of heterogeneity in fuels (*e.g.*, Yokelson et al., 2013; Hodshire et al., 2019). Only very few studies have reported EF_{NH_3} derived from measurements carried out in the field (*e.g.*, Lindaas et al., 2021).

55 The limited availability of field data is mostly because NH$_3$ is difficult to measure. NH$_3$ is a "sticky" molecule that easily adsorbs onto inlet and instrumental surfaces. This makes fast airborne measurements of NH$_3$ particularly challenging. Müller et al. (2014; see Supplement) have shown that proton-transfer-reaction time-of-flight mass spectrometry (PTR-ToF-MS) can be used for airborne NH$_3$ measurements, although with some limitations tied to a relatively slow time response and a poor detection limit due to a large intrinsic background. The University of Innsbruck PTR-ToF-MS instrument has been used for

60 airborne measurements of NH$_3$ in previous studies (Sun et al., 2015; Kelly et al., 2018; Guo et al., 2021; Da Pan et al., 2021).

The Fire Influence on Regional to Global Environments and Air Quality (FIREX-AQ) study was a joint NOAA/NASA effort to investigate the atmospheric impact of wildfires and agricultural fires in the contiguous US (Warneke et al., 2022). In summer 2019, the NASA DC-8 Airborne Science Laboratory performed *in situ* measurements in smoke plumes emitted from wildfires in the Western US and agricultural fires in the Southeastern US. The aircraft payload included a PTR-ToF-MS instrument that

65 was modified and optimized for the fast measurement of NH$_3$. It also included an aerosol mass spectrometer (AMS) for fast measurement of submicron particulate ammonium (NH$_4^+$). This allowed us to measure and report a set of emission factors of NH$_3$ and NH$_x$, with NH$_x$ = NH$_3$ + NH$_4^+$, for different types of fires.

2 Methods

2.1 FIREX-AQ

70   The FIREX-AQ experiment has been described in detail by Warneke et al. (2022). During the 2019 field campaign, NH_3 and
NH_4^+ were measured aboard the NASA DC-8 in smoke plumes emitted from six wildfires in the Western US (Shady, Williams
Flats, Castle, Ridge Top, Mica/Lick Creek, Horsefly), two prescribed grassland fires in the Central US (Hickory Ridge State
Wildlife Management Area, Tallgrass Prairie National Preserve), and one prescribed forest fire in the Southern US (Black
Water River State Forest). A map showing the location of these fires is given in the Supplement (Fig. S1). Vegetation and fuel
75   type information is summarized in Tab. S1. Several downwind transects were typically flown in the smoke plumes emitted
from the wildfires. In addition, the NASA DC-8 sampled smoke plumes from a large number of agricultural fires in the
Southeastern US. These small plumes were typically sampled twice in perpendicular direction. We successfully measured NH_3
and NH_4^+ in plumes emitted from 66 agricultural fires.

2.2 Instrumentation

80   A modified PTR-ToF-MS instrument was used for fast-response measurements of NH_3 aboard the NASA DC-8 during FIREX-
AQ. The airborne PTR-ToF-MS analyzer has been described in detail by Müller et al. (2014). Only the modifications pertinent
to the fast measurement of NH_3 are thus described here.

For reducing the instrumental NH_3 background, 12-25 standard cubic centimeters per minute (sccm; "standard" herein means
referenced to a temperature of 273.15 K and a pressure of 101325 Pa) of ultra-pure helium (6.0; Praxair Inc., Danbury, CT,
85   US) were introduced into the source drift region between the drift tube and the ion source. This reduced the backflow of
nitrogen into the plasma region and suppressed NH_3 formation in the plasma (Müller et al., 2020, and references therein). The
instrumental NH_3 background was thereby reduced from triple digit to low single digit ppb levels.

For improving the instrumental time response to NH_3, all stainless-steel parts in the drift tube were surface-passivated with a
functionalized hydrogenated amorphous silicon coating (Piel et al., 2021), and the drift tube was heated to 120 °C. Surface
90   passivation and heating significantly reduces the adsorption of NH_3 to instrumental surfaces, lowering the instrumental
response time to ~2 seconds (see Figure 4 of Piel et al., 2021).

A series of inlet configurations were tested during the initial phase of the FIREX-AQ campaign. The fastest response to NH_3
was achieved when air was sampled at a flow rate of ~60 standard liters per minute (slpm) through a heated Teflon PFA tube
(length: ~2 m, inner diameter: 3.96 mm, wall temperature: 60 °C). Evaporation of ammonium nitrate particles in the main
95   sampling line was not investigated, but is believed to be small due to the short sample residence time (<25 ms). For inertially
separating particles from the analyte air, a small flow was subsampled from the main inlet line in rearward direction and
directed into the drift tube through a Teflon PFA tube (length: ~10 cm, outer diameter: 3.175 mm, temperature: 120 °C). The
subsampling flow was set to ~250 sccm via a pinch valve applied on the PFA tube. An NH_3 time response of a few seconds
was ultimately achieved (see Results section).

3

100 Since in-field calibrations with different methods (NH_3 in N_2 standard gas cylinder, permeation calibration device, cross-calibration with a Picarro G2103 NH_3 analyzer) were inconsistent, we carried out an extensive post-mission NH_3 calibration in the laboratory. For that purpose, an artificial atmosphere (NH_3 in air) was generated in a 250 L environmental ("smog") chamber equipped with a Fourier Transform Infrared (FT-IR) spectrometer (Bruker IFS 66v/S). The concentrations of NH_3 (accuracy: ± 5 %) were determined from the FT-IR spectra (120 m path length, 0.125 cm^{-1} spectral resolution) in a global non-

105 linear least squares spectral fitting procedure (Griffith, 1996) employing the absolute cross sections of NH_3 (Gordon et al., 2017). The estimated accuracy of the reported NH_3 mixing ratios is ± 15 %. We note that this accuracy estimate is not valid when NH_3 mixing ratios abruptly changed and inlet/instrument surfaces were not equilibrated.

Submicrometer (50% cutoff size for a vacuum aerodynamic diameter ~1 µm (about 850 nm geometric diameter for most fire plumes based on in-field calibrations) NH_4^+ was measured by an Aerodyne high-resolution time-of-flight AMS instrument

110 (DeCarlo et al., 2006; Canagaratna et al., 2007), with a time resolution of up to 10 Hz time. The accuracy (2σ) of the NH_4^+ data is estimated to be ± 34 % (Bahreini et al., 2009), while the detection limit was typically much smaller (25 ppt at 1 Hz in clean air, ~200 ppt in fire plumes). The inlet flow was optimized to allow for near real time sampling (0.3 s residence time) and to minimize particle volatilization in the inlet. We note that, based on the current state of knowledge, the AMS NH_4^+ data collected in fresh smoke plumes suffer from a minor (≤ 20%) positive interference from reduced organic nitrogen compounds.

115 A general correction is still under development based on positive matrix factorization (PMF) analysis.

Carbon monoxide (CO) and methane (CH_4) were measured by the Differential Absorption Carbon Monoxide Measurement (DACOM) instrument (Sachse et al., 1991), which is based on mid-infrared wavelength modulation spectroscopy. The uncertainty in the CO data is 2.1 ± 0.2 ppb; the uncertainty for CH_4 is about 1 %. Carbon dioxide (CO_2) was measured by a LICOR model 7000 analyzer (Vay et al., 2009), which is based on nondispersive infrared absorption spectroscopy. For $CO_2 <$

120 500 ppm, the accuracy is 0.25 ppm and the precision is 0.1 ppm, while for higher mixing ratios the total uncertainty is about 2 %. Information about fuel types was obtained from the 30 m Fuel Characteristic Classification System (FCCS; Ottmar et al., 2007), the 30 m Cropland Data Layer classification 2019 dataset, and ground intelligence.

2.3 Emission factor, modified combustion efficiency

We used the carbon mass balance method for calculating EF_{NH_3} (Yokelson et al., 1996; 1999). The underlying assumption is

125 that the carbon in the fire fuel is predominantly emitted as CO_2, CO and CH_4. EF_{NH_3} (in g kg^{-1}) is thus described by the simplified equation (1):

$$EF_{NH_3} = \frac{\Delta NH_3}{\Delta CO_2 + \Delta CH_4 + \Delta CO} \times \frac{17}{12} \times F_c \times 1000 \quad (1)$$

Δ is the above background mixing ratio in the plume of the respective trace gas, 17 is the molar mass of NH_3 (in g mol^{-1}), and 12 is the molar mass of carbon (in g mol^{-1}). F_c is the fraction of carbon in the fuel, which we assumed to be 0.5 (Yokelson et

130 al., 1999).

A problem in the calculation of EF_{NH_3} arises from the fact that NH_3 is a "sticky" compound. When the aircraft first penetrates a smoke plume, NH_3 molecules typically adsorb onto inlet and instrumental surfaces, thereby delaying the signal response of the analyzer. When the airplane exits the plume, the desorbing NH_3 molecules cause a signal tailing (Figure S2a). For calculating Δ, we thus applied the method described in the Supplement of Müller et al. (2016) and calculated cumulative volume mixing ratios including the period after the plume encounter when the NH_3 signal tailed off (Figure S2b). The signal tailing was particularly pronounced during the initial phase of the campaign (before 24 August 2019) when the inlet configuration had not yet been optimized. NH_x is the sum of NH_3 and NH_4^+; EF_{NH_x} was calculated as the sum of EF_{NH_3} and $EF_{NH_4^+}$. The modified combustion efficiency (MCE) was calculated as $\Delta CO_2/(\Delta CO_2+\Delta CO)$.

Data from 180 plume transects were included in our analysis of the wildfire emissions. We only used data from plume transects in which CO mixing ratios exceeded 300 ppb for more than 20 seconds and from plumes in which MCE values were stable (standard deviation of MCE < 0.05). Data from seven plume transects were excluded due to missing NH_3, NH_4^+ or CH_4 data. Our EF analysis was not based on a single plume transect in closest proximity to the wildfire, as we observed in several plumes that $\Delta NH_3/\Delta CO$ increased during a few initial downwind transects (see Fig. S3). The reason for this increase (typically <15%) is unclear. We thus included all plume transects in our analysis, up to where $\Delta NH_3/\Delta CO$ reached its maximum and derived an average EF_{NH_3} and EF_{NH_x} (± standard deviation, SD). Data from 164 plume transects were included in our analysis of the agricultural fire emissions. Data from 12 plume transects were excluded due to missing NH_3 or NH_4^+ data.

3 Results and Discussion

3.1 Airborne measurements of NH_3 in smoke plumes

Figure 1a shows the mixing ratio of NH_3 (in red) as measured by the PTR-ToF-MS instrument on 7 August 2019 aboard the NASA DC-8. The aircraft flew nine downwind transects at an altitude of 5160 m above sea level (ASL) for sampling the plume emitted from the Williams Flats Fire in Washington State. The NH_3 signal increased with CO (in black) when the plane entered the plume, exhibited a similar time trend as CO within the plume and decreased to background levels outside the plume, although with some tailing (few minutes). NH_3 maxima ranged from 110 to 200 ppb, which were typical maximum NH_3 levels measured in fire plumes throughout the 2019 FIREX-AQ field campaign. Also shown in Figure 1a is the time trace of NH_4^+ (in dark yellow) as measured by the AMS instrument, with maximum mixing ratios ranging from 42 to 65 ppb. The observation of significant amounts of NH_4^+ indicates that NH_4^+ was primary emitted (as for example observed by Lewis et al., 2009) and/or gaseous NH_3 had been partly converted to particulate NH_4^+ by the time of sampling (≥2 h after emission). A rapid conversion can be caused by the fast reaction of NH_3 with primary emitted acids such as hydrochloric acid (HCl), nitric acid (HNO_3) and organic acids, or occur more slowly downwind via the reaction of NH_3 with secondary formed acids.

5

160   Figure 1b shows the mixing ratios of NH_3, NH_4^+ and CO as observed when the NASA DC-8 crossed a plume emitted from a

small cornfield fire in the Mississippi River Valley on 26 August 2019 at an altitude of 325 m ASL. All data are shown at the

frequency they were recorded (5 Hz), which resulted in an increased noise for NH_3. The tailing was however reduced to a few

seconds with the improved PTR-ToF-MS inlet. We show the 5-Hz data for demonstrating that we succeeded in measuring

such small fire plumes from a jet aircraft. For further analysis, we used the 1 second integrated data. Notably, the AMS

165   instrument detected significant amounts of NH_4^+ in this very fresh plume, indicating that either direct emission from the fire

or a rapid conversion of NH_3 to NH_4^+ had occurred. The latter could be caused by the fast reaction of NH_3 with HCl, which is

emitted in significant amounts from agricultural fires (Liu et al., 2017). Another plausible explanation is the resuspension of

recently applied ammonium nitrate fertilizer.
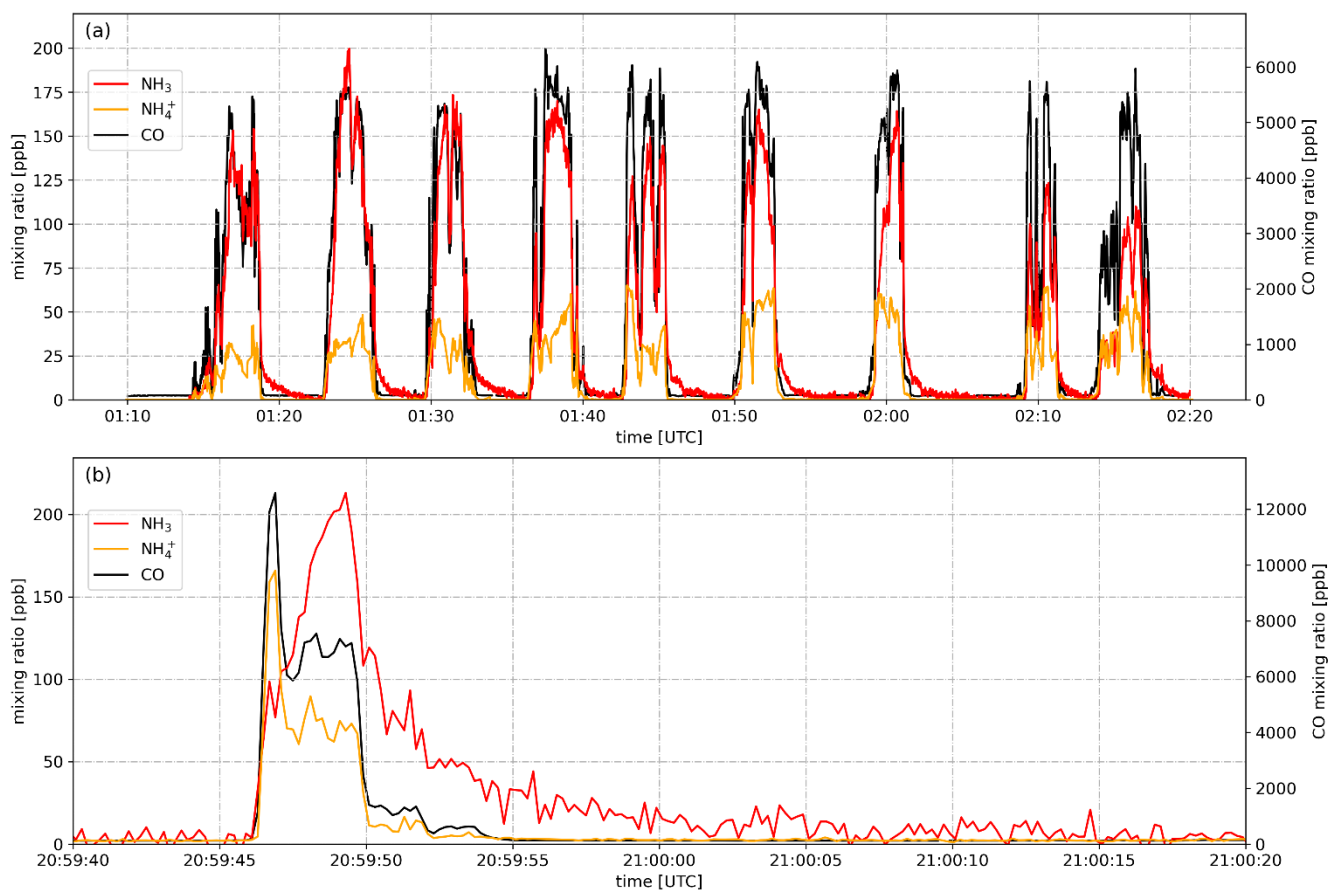
170   **Figure 1: Mixing ratios of NH_3, NH_4^+, and CO as measured when the NASA DC-8 transected (a) the plume emitted from the Williams Flats Fire on 7 August, 2019 in downwind direction and (b) the plume emitted from a small corn field fire in the Mississippi River Valley on 26 August, 2019.**

Due to the fact that NH_4^+ was already present in very fresh smoke (due to direct emission or rapid conversion), we will herein

175   also report EF_{NH_x}, as suggested in previous work by Hegg et al. (1990). In Figure 2a, we plot EF_{NH_x} against EF_{NH_3} for the six

Western US wildfires investigated during the 2019 FIREX-AQ field campaign. The two EFs are highly correlated ($R^2 = 0.96$),

with the slope of the linear regression curve being close to unity (1.07 ± 0.05). This regression analysis suggests that NH_4^+

added ~0.5 g kg^{-1} (offset of the regression line: 0.47 ± 0.11) to EF_{NH_x} throughout the campaign. The offset may be interpreted

as the typical direct NH_4^+ emission factor (or fast conversion of NH_3).

180   In the case of the agricultural burns, the NASA DC-8 sampled the plumes in very close proximity to the fires. EF_{NH_x} and

EF_{NH_3} had again a regression slope of ~1. The offset was mainly caused by elevated NH_4^+ emissions and low NH_3 emissions

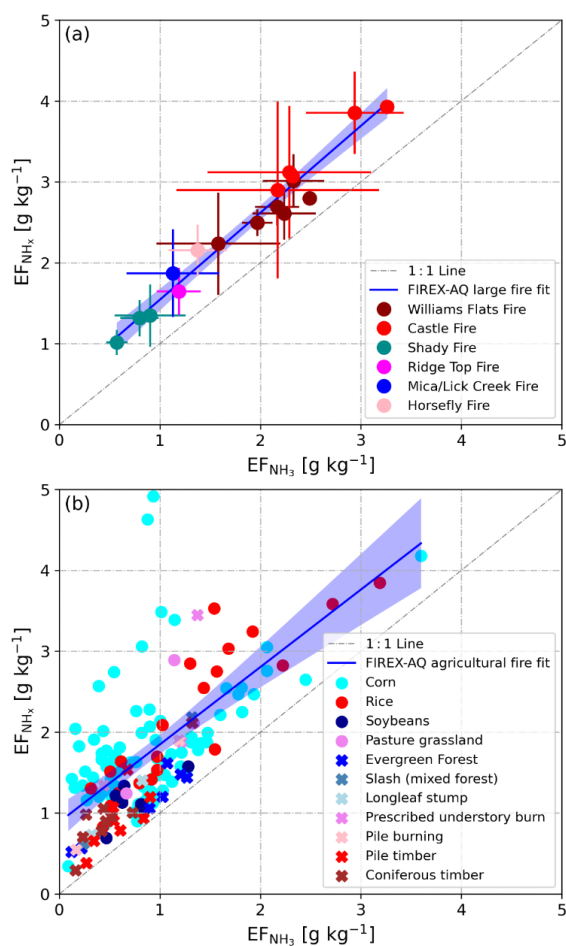from some of the cornfield fires (Fig. 2b).

Figure 2: EF_{NH_x} *vs.* EF_{NH_3} **as derived from** *in situ* **measurements in the plumes of (a) six wildfires and (b) 66 small**

185   **agricultural fires (circles: field-dominated fuels, crosses: timber-dominated fuels; see section 3.3 for details)**

3.2 NH₃ and NHₓ emissions from wildfires in the Western US

In situ measurements of NH_3 and NH_4^+ were made in smoke plumes emitted from six wildfires in the Western US. Table 1 provides a detailed overview of EF_{NH_3} and EF_{NH_x} derived from these measurements. Plumes from the Shady, Williams Flats and Castle Fires were sampled multiple times and we list the data from each of the sampling patterns as well as the average value. EF_{NH_3} and EF_{NH_x} were lowest for the Shady Fire. The low emissions may be caused by the difference in fuels, which in the case of the Shady Fire was modified or managed xeric understory (Tab. S1).

Table 1: EF_{NH_3} and EF_{NH_x} derived from *in situ* measurements in the plumes of 6 wildfires in the Western US.

			EF_{NH_3} (g kg⁻¹)		EF_{NH_x} (g kg⁻¹)		MCE	
Name	State	Date (dy.mo.yr)	mean	SD	mean	SD	mean	SD
Shady 1st pattern	ID	25.07.2019	0.57	0.11	1.02	0.15	0.906	0.003
Shady 2nd pattern	ID	25.07.2019	0.80	0.19	1.32	0.23	0.892	0.007
Shady 3rd pattern	ID	25.07.2019	0.90	0.35	1.35	0.39	0.887	0.029
Shady mean			**0.76**	**0.22**	**1.23**	**0.26**	**0.895**	**0.013**
Williams Flats 1st pattern	WA	03.08.2019	1.58	0.62	2.24	0.63	0.908	0.003
Williams Flats 2nd pattern	WA	03.08.2019	2.24	0.32	2.61	0.33	0.907	0.005
Williams Flats	WA	06.08.2019	2.33	0.31	3.01	0.33	0.894	0.004
Williams Flats 1st pattern	WA	07.08.2019	2.49	0.07	2.80	0.09	0.905	0.004
Williams Flats 2nd pattern	WA	07.08.2019	1.97	0.15	2.50	0.16	0.909	0.001
Williams Flats 3rd pattern	WA	07.08.2019	2.17	--	2.69	--	0.901	0.001
Williams Flat mean			**2.13**	**0.28**	**2.64**	**0.29**	**0.904**	**0.003**
Castle 1st pattern	AZ	12.08.2019	2.29	0.81	3.12	0.82	0.884	0.003
Castle 2nd pattern	AZ	12.08.2019	2.94	0.49	3.85	0.51	0.890	0.002
Castle longitudinal transect	AZ	12.08.2019	2.32	--	3.07	--	0.864	--
Castle 1st pattern	AZ	13.08.2019	2.17	1.01	2.90	1.09	0.895	0.007
Castle 2nd pattern	AZ	13.08.2019	3.26	--	3.93	--	0.892	--
Castle mean			**2.60**	**0.77**	**3.37**	**0.81**	**0.885**	**0.004**
Ridge Top	MT	02.08.2019	1.19	0.22	1.65	0.29	0.940	0.011
Mica/Lick Creek	ID	02.08.2019	1.13	0.46	1.87	0.54	0.913	0.021
Horsefly	MT	06.08.2019	1.38	0.29	2.15	0.32	0.859	0.010

Average EF_{NH_3} and EF_{NH_x} values for the six wildfires in the Western US were 1.86 ± 0.75 g kg⁻¹ and 2.47 ± 0.80 g kg⁻¹, respectively. We compare our results to those obtained in two recent studies. Lindaas et al. (2021) investigated NH₃ emissions from wildfires in the Western US during the 2018 WE-CAN campaign. We calculated an average EF_{NH_3} of 1.48 ± 0.91 g kg⁻

[1] for the WE-CAN data. This is slightly lower than the average EF_{NH_3} reported herein, but within the combined uncertainties of the two methods: ±12% for the quantum-cascade tunable infrared laser direct absorption spectrometer (QC-TILDAS) used during WE-CAN, and ±15% for the PTR-ToF-MS analyzer used during FIREX-AQ. Selimovic et al. (2018) investigated

200   emissions from fires fueled by a wide range of US vegetation types in the FIREX FireLab 2016 laboratory study. We only used the data for FIREX-AQ relevant fuels (see Table S1) and obtained a significantly lower average EF_{NH_3} of 0.67 ± 0.38 g kg^{-1} for the FIREX FireLab data. This finding seems to confirm that laboratory fires do not realistically simulate wildfires (*e.g*., Yokelson et al., 2013, Hodshire et al., 2019) and thereby underestimate real-world emissions of NH_3.

In Figure 3, we plot the measured EF_{NH_3} values (6 wildfires, multiple sampling of 3 fires) as a function of MCE along with

205   trends from the WE-CAN and FIREX FireLab studies. In the case of the FIREX-AQ data (regression line and confidence band in blue), EF_{NH_3} and MCE correlated poorly, with Pearson's coefficient of determination (R^2) being only 0.04. As opposed to the WE-CAN study (regression line and confidence band in black) and the FIREX FireLab experiments (regression line and confidence band in dark yellow), we did not find a clear inversion correlation between MCE and NH_3 emissions.
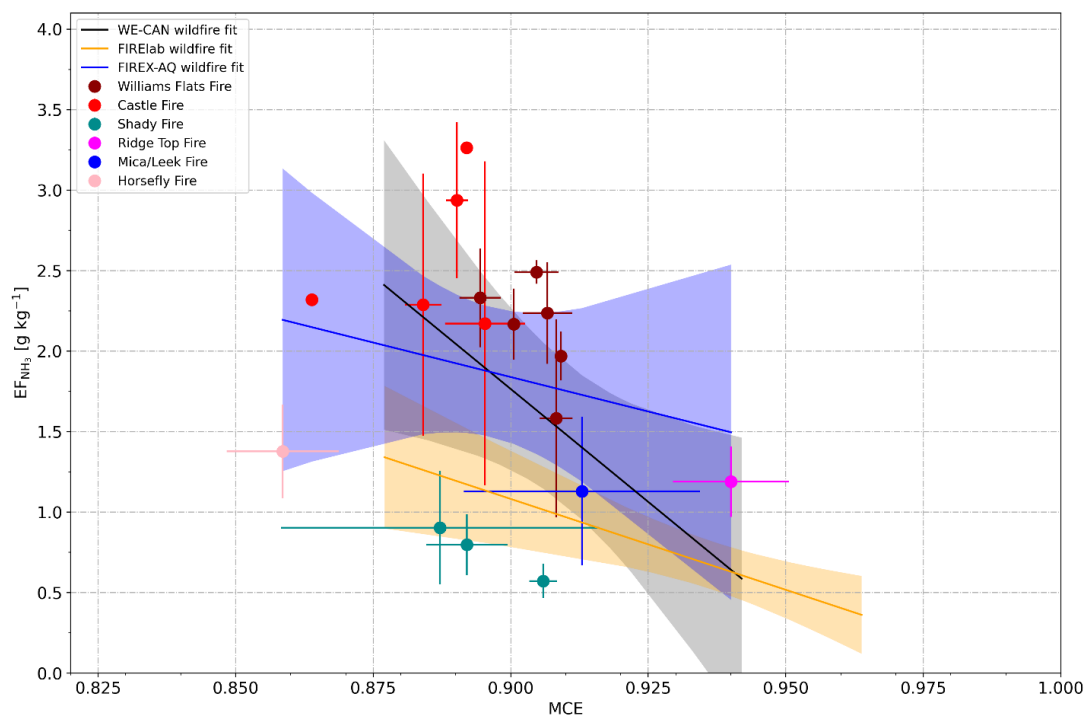
210   **Figure 3: Scatter plot of EF_{NH_3} (as measured for six Western US wildfires during FIREX-AQ and obtained from two literature sources) *vs*. MCE.**

Finally, we would like to discuss the results presented by Gkatzelis et al. (2022), who provide an overview of EFs derived from the 2019 FIREX-AQ data. Their analysis yielded an average EF_{NH_3} of 1.15 ± 0.79 g kg^{-1}, which is significantly lower

than the average value we have presented herein. This discrepancy can be explained by the fact that Gkatzelis et al. (2022) did

215 not include the additional contribution from the NH₃ signal tailing outside the plume, nor did it include data from multiple

plume transects downwind of the fire. The fact that different analyses of the same data result in significantly different EF_{NH_3}

highlights the fact that data comparisons between different studies need to be interpreted with caution.

3.3 NH₃ and NHₓ emissions from agricultural fires in the Southeastern US

In situ measurements of NH₃ and NH₄⁺ were made in smoke plumes emitted from 66 small agricultural fires in the Southeastern

220 US. EF_{NH_3} values varied widely, covering a range from 0.09 to 3.60 g kg⁻¹. The following average values and standard

deviations were derived: $EF_{NH_3} = 0.89 \pm 0.58$ g kg⁻¹, $EF_{NH_x} = 1.74 \pm 0.92$ g kg⁻¹, MCE = 0.92 ± 0.04.

We grouped the agricultural fuels into field-dominated and timber-dominated fuels. The field-dominated fuels include corn,

rice, soybeans, and grassland pasture. The timber-dominated fuels include evergreen forest, coniferous timber, prescribed

understory fire, pile burning, slash burning, pile timber slash mixture burns, and pile burning of longleaf pine tree stumps.

225 Table 2 lists EF_{NH_3}, EF_{NH_x} and MCE for the two main categories and 11 subcategories.

Table 2: EF_{NH_3}, EF_{NH_x} and MCE as measured during FIREX-AQ for small agricultural fires in the Southeastern US burning on different types of fuel.

		EF_{NH_3} (g kg⁻¹)		EF_{NH_x} (g kg⁻¹)		MCE	
Fuel type	66	mean	SD	mean	SD	mean	SD
Corn	33	0.90	0.58	1.85	0.78	0.937	0.023
Rice	11	1.21	0.74	2.13	0.93	0.897	0.057
Soybean	4	0.75	0.27	1.16	0.27	0.925	0.024
Grassland Pasture	2	1.05	0.34	2.08	0.82	0.824	0.109
Field-dominated average	**50**	**0.95**	**0.60**	**1.92**	**0.92**	**0.926**	**0.042**
Evergreen Forest	1	0.83	0.47	1.13	0.44	0.914	0.027
Pile burning (mixed)	4	0.51	0.47	1.12	0.62	0.920	0.042
Slash burn (mixed forest)	2	0.78	0.76	1.40	1.10	0.918	0.063
Prescribed understory burn	1	1.39	0.19	2.67	1.11	0.864	0.022
Pile timber slash	5	0.58	0.21	0.95	0.33	0.858	0.060
Pile longleaf pine tree stump	1	0.57	0.35	1.07	0.48	0.877	0.004
Timber slash coniferous	2	0.51	0.35	0.98	0.49	0.912	0.019
Timber-dominated average	**16**	**0.67**	**0.42**	**1.19**	**0.68**	**0.896**	**0.045**

The data listed in Table 2 indicate that field-dominated fuels emit more NH₃ and NHₓ than timber-dominated fuels. Agricultural

230 areas are usually nitrogen-fertilized, which may cause increased NH₃ emissions. EF_{NH_x} is roughly a factor of two higher than

EF_{NH_3}, which indicates higher primary NH₄⁺ emissions and/or a very rapid NH₃ to NH₄⁺ conversion in these fresh plumes.

Figure 4 shows EF_{NH_3} as a function of MCE for different fuels (as measured in individual fires), the averages derived for field-dominated fuels and timber-dominated fuels and the results from four previous studies (McMeeking et al., 2009; Stockwell et al., 2015; Müller et al., 2016; Selimovic et al., 2018). Also in this case, EF_{NH_3} and MCE correlated poorly with R^2 being 0.05. The literature values match the low NH_3 emissions (< 1 g kg^{-1}) we observed for most agricultural fires, but the high NH_3 emissions from burning rice and corn residues have not been reported before.
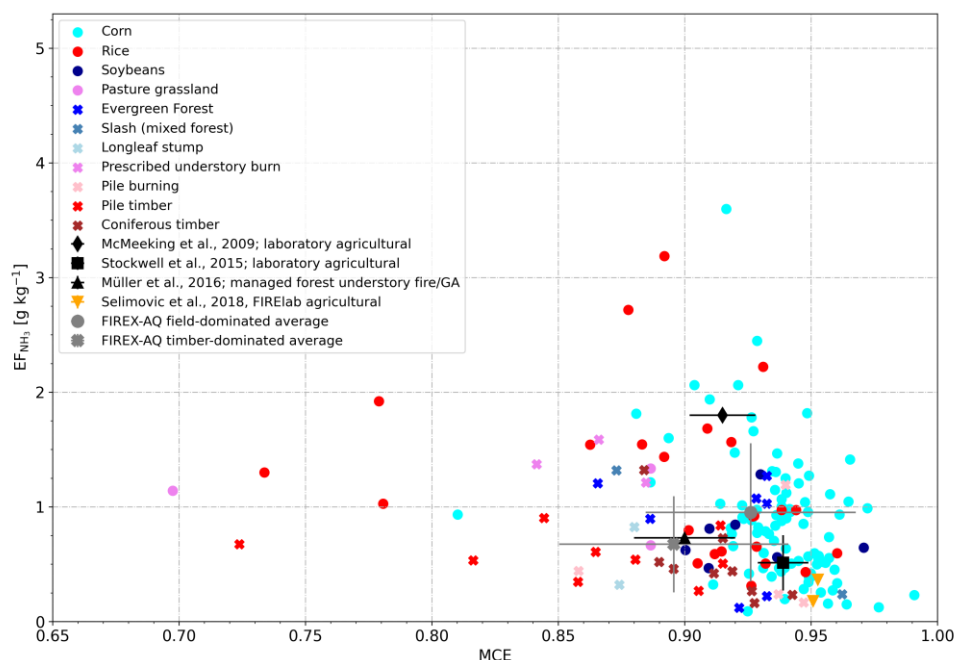
Figure 4: Scatter plot of EF_{NH_3} *vs.* MCE as measured for 66 agricultural fires (circles: field-dominated fuels, crosses: timber-dominated fuels) and obtained from four literature sources.

3.4 NH$_3$ and NH$_x$ emissions from other fires

We also measured NH_3 and NH_4^+ in smoke plumes emanating from two prescribed grassland fires in the Central US and one prescribed forest fire in the Southern US. These fires do not fall within the two main categories discussed in the previous two sections and are thus separately presented here. Table 3 lists the fire details, EF_{NH_3}, EF_{NH_x} and MCE for these three fires.

245 **Table 3: EF_{NH_3}, EF_{NH_x} and MCE as measured during FIREX-AQ for two prescribed grassland fires in the Central US and one prescribed forest fire in the Southern US.**

Fire details	EF_{NH_3} (g kg^{-1})		EF_{NH_x} (g kg^{-1})		MCE	
	mean	SD	mean	SD	mean	SD
Hickory Ridge State Wildlife Management Area prescribed, 29.08.2019, NE grass during the green growing season (not dry)	0.33	0.12	1.19	0.93	0.907	0.002
Tallgrass Prairie National Preserve prescribed, 29.08.2019, KS prairie tallgrass during the green growing season (not dry)	0.92	0.20	1.73	0.49	0.894	0.014
Black Water River State Forest prescribed, 30.08.2019, FL oak, mature longleaf pine, mesic and xeric shrub, grass, litter, understory	0.30	0.16	0.61	0.20	0.942	0.006

4 Conclusions

During the 2019 FIREX-AQ field campaign, we measured NH$_3$ and NH$_4^+$ aboard the NASA DC-8 in wildfire and agricultural fire plumes. We found that NH$_4^+$ was either directly emitted from the fire (consistent with past laboratory experiments) and/or

250 NH$_3$ had already partially partitioned to particulate NH$_4^+$ at the time of sampling. We thus also evaluated emissions of NH$_x$ and produced a comprehensive set of EF_{NH_3} and EF_{NH_x} for wildfires in the Western US and agricultural fires in the Southeastern US. Our data show no clear inverse correlation between MCE and EF_{NH_3}. EF_{NH_3} values measured in plumes of large wildfires were similar to measurements of past field studies, but significantly higher than observed in prior work on laboratory simulated fires, which typically burn on a single fuel. We also report the first extensive set of field measurement

255 derived EF_{NH_3} and EF_{NH_x} values for different types of agricultural fires in the Southeastern US. NH$_3$ emissions were highest from fires of corn and rice residues, which may be caused by fertilization of these fields. Substantial amounts of NH$_4^+$ were detected in freshly emitted smoke from some of the corn and rice field fires, which warrants further investigation.

Data availability

260 All the FIREX-AQ data are available at NASA's Atmospheric Science Data Center (DOI: 10.5067/SUBORBITAL/FIREXAQ2019/DATA001) (NASA, 2019).

Author contribution

LT supported the PTR-ToF-MS instrument development, performed the field measurements, performed the data analysis and interpretation, and wrote the manuscript draft. TM built and characterized the modified PTR-ToF-MS instrument and

265 performed field measurements. FP performed field and laboratory measurements and supported the data analysis as well as the PTR-ToF-MS instrument development. CJN supported the post-mission calibration experiments. PCJ, HG, BAN, MSK and JLJ provided the NH_4^+ data. HH, GD, JPD, JBN provided the CO_2, CO and CH_4 data. EBW, EG and AJS provided the fuel characterization information. AW conceived the modified PTR-ToF-MS instrument, supervised the measurements and data analysis, performed field measurements and finalized the manuscript. All authors commented and accepted the final

270 version of the manuscript.

Conflicts of interest

The authors declare no conflict of interest.

Acknowledgements

References

Akagi, S. K., Yokelson, R. J., Wiedinmyer, C., Alvarado, M. J., Reid, J. S., Karl, T., Crounse, J. D., Wennberg, P. O. (2011). Emission factors for open and domestic biomass burning for use in atmospheric models. *Atmos. Chem. Phys., 11*(9), 4039-4072. doi:10.5194/acp-11-4039-2011

285 Andreae, M. O. (2019). Emission of trace gases and aerosols from biomass burning – an updated assessment. *Atmos. Chem. Phys., 19*(13), 8523-8546. doi:10.5194/acp-19-8523-2019

Andreae, M. O., & Merlet, P. (2001). Emission of trace gases and aerosols from biomass burning. *Global biogeochemical cycles, 15*(4), 955-966. doi:https://doi.org/10.1029/2000GB001382

Bahreini, R., Ervens, B., Middlebrook, A. M., Warneke, C., de Gouw, J. A., DeCarlo, P. F., Jimenez, J. L., Brock, C. A.,

290 Neuman, J. A., Ryerson, T. B., Stark, H., Atlas, E., Brioude, J., Fried, A., Holloway, J. S., Peischl, J., Richter, D., Walega, J., Weibring, P., Wollny, A. G., Fehsenfeld, F. C. (2009). Organic aerosol formation in urban and industrial plumes near Houston and Dallas, Texas. *Journal of Geophysical Research: Atmospheres, 114*(D7). doi:https://doi.org/10.1029/2008JD011493

Bobbink, R., & Hicks, W. K. (2014). Factors Affecting Nitrogen Deposition Impacts on Biodiversity: An Overview. In M. A.

295 Sutton, K. E. Mason, L. J. Sheppard, H. Sverdrup, R. Haeuber, & W. K. Hicks (Eds.), *Nitrogen Deposition, Critical Loads and Biodiversity* (pp. 127-138). Dordrecht: Springer Netherlands.

Burling, I. R., Yokelson, R. J., Griffith, D. W. T., Johnson, T. J., Veres, P., Roberts, J. M., Warneke, C., Urbanski, S. P., Reardon, J., Weise, D. R. (2010). Laboratory measurements of trace gas emissions from biomass burning of fuel types from the southeastern and southwestern United States. *Atmos. Chem. Phys., 10*(22), 11115-11130. doi:10.5194/acp-

300 10-11115-2010

Canagaratna, M. R., Jayne, J.T., Jimenez, J.L., Allan, J.D., Alfarra, M.R., Zhang, Q., Onasch, T.B., Drewnick, F., Coe, H., Middlebrook, A., Delia, A., Williams, L.R., Trimborn, A.M., Northway, M.J., DeCarlo, P.F., Kolb, C.E., Davidovits,

P., Worsnop, D.R. (2007). Chemical and microphysical characterization of ambient aerosols with the aerodyne aerosol mass spectrometer. *Mass Spectrometry Reviews, 26*(2), 185-222. doi:https://doi.org/10.1002/mas.20115

305 DeCarlo, P. F., Kimmel, J. R., Trimborn, A., Northway, M. J., Jayne, J. T., Aiken, A. C., Gonin, M., Fuhrer, K., Horvath, T., Docherty, K. S., Worsnop, D. R., Jimenez, J. L. (2006). Field-Deployable, High-Resolution, Time-of-Flight Aerosol Mass Spectrometer. *Analytical Chemistry, 78*(24), 8281-8289. doi:10.1021/ac061249n

Gkatzelis, G. I., Coggon, M. M., Stockwell, C. E., Hornbrook, R. S., Allen, H., Apel, E.C., Bela, M. M., Blake, D. R., Bourgeois, I., Brown, S. S., Campuzano-Jost, P., Clair, J. M. St., Crawford, J. H., Crounse, J. D., Day, D. A., DiGangi,
310 J. P., Diskin, G. S., Fried, A., Gilman, J. B., Guo, H., Hair, J.W., Halliday, H. S., Hanisco, T. F., Hannun, R., Hills, Al., Huey, L. G., Jimenez, J. L., Katich, J. M., Lamplugh, A., Lee, Y. R., Liao, J., Lindaas, J., McKeen, S. A., Mikoviny, T., Nault., B. A., Neuman, J. A., Nowak, J. B., Pagonis, D., Peishcl, J., Perring, A. E., Piel, F., Rickly, P. S., Robinson, M. A., Rollins, A. W., Ryerson, T. B., Schueneman, M. K., Schwantes, R. H., Schwarz, J. P., Sekimoto, K., Selimovic, V., Shingler, T., Tanner, D. J., Tomsche, L., Vasquez, K. T., Veres, P. R., Washenfelder, R., Weibring,
315 P., Wennberg, P. O., Wisthaler, A., Wolfe, G. M., Womack, C. C.,, Xu, l., Yokelsom, R. J., Warneke, C. (2022). Parametrications of US wildfire and prescribed fire emission ratios and emission factors based on FIREX-AQ aircraft measurements. *in preparation*.

Goode, J. G., Yokelson, R. J., Susott, R. A., & Ward, D. E. (1999). Trace gas emissions from laboratory biomass fires measured by open-path Fourier transform infrared spectroscopy: Fires in grass and surface fuels. *Journal of Geophysical*
320 *Research: Atmospheres, 104*(D17), 21237-21245. doi:https://doi.org/10.1029/1999JD900360

Gordon, I. E., Rothman, L. S., Hill, C., Kochanov, R. V., Tan, Y., Bernath, P. F., Birk, M., Boudon, V., Campargue, A., Chance, K. V., Drouin, B. J., Flaud, J. M., Gamache, R. R., Hodges, J. T., Jacquemart, D., Perevalov, V. I., Perrin, A., Shine, K. P., Smith, M. A. H., Tennyson, J., Toon, G. C., Tran, H., Tyuterev, V. G., Barbe, A., Csaszar, A. G., Devi, V. M., Furtenbacher, T., Harrison, J. J., Hartmann, J. M., Jolly, A., Johnson, T. J., Karman, T., Kleiner, I.,
325 Kyuberis, A. A., Loos, J., Lyulin, O. M., Massie, S. T., Mikhailenko, S. N., Moazzen-Ahmadi, N., Muller, H. S. P., Naumenko, O. V., Nikitin, A. V., Polyansky, O. L., Rey, M., Rotger, M., Sharpe, S. W., Sung, K., Starikova, E., Tashkun, S. A., Vander Auwera, J., Wagner, G., Wilzewski, J., Wcislo, P., Yu, S., and Zak, E. J. (2017). The HITRAN2016 molecular spectroscopic database. *J. Quant. Spectrosc. Radiat. Transfer, 203*, 3-69. doi:10.1016/j.jqsrt.2017.06.038

330 Griffith, D. W. (1996). Synthetic calibration and quantitative analysis of gas-phase FT-IR spectra. *Applied spectroscopy, 50*(1), 59-70.

Guo, H., Campuzano-Jost, P., Nault, B. A., Day, D. A., Schroder, J. C., Kim, D., Dibb, J. E., Dollner, M., Weinzierl, B., Jimenez, J. L. (2021). The importance of size ranges in aerosol instrument intercomparisons: a case study for the Atmospheric Tomography Mission. *Atmos. Meas. Tech., 14*(5), 3631-3655. doi:10.5194/amt-14-3631-2021

335 Hegg, D. A., Radke, L. F., Hobbs, P. V., Rasmussen, R. A., Riggan, P. (1990). Emissions of some trace gases from biomass fires. *Journal of Geophysical Research: Atmospheres, 95*(D5), 5669-5675. doi:https://doi.org/10.1029/JD095iD05p05669

Hodshire, A. L., Akherati, A., Alvarado, M. J., Brown-Steiner, B., Jathar, S. H., Jimenez, J. L., Kreidenweis, S. M., Lonsdale, C. R., Onasch, T. B., Ortega, A. M., Pierce, J. R. (2019). Aging Effects on Biomass Burning Aerosol Mass and
340 Composition: A Critical Review of Field and Laboratory Studies. *Environmental Science & Technology, 53*(17), 10007-10022. doi:10.1021/acs.est.9b02588

Kelly, J. T., Parworth, C. L., Zhang, Q., Miller, D. J., Sun, K., Zondlo, M. A., Baker, K. R., Wisthaler, A., Nowak, J. B., Pusede, S. E., Cohen, R. C., Weinheimer, A. J., Beyersdorf, A. J., Tonnesen, G. S., Bash, J. O., Valin, L. C., Crawford, J.H., Fried, A., Walega, J.G. (2018). Modeling NH4NO3 Over the San Joaquin Valley During the 2013 DISCOVER-
345 AQ Campaign. *Journal of Geophysical Research: Atmospheres, 123*(9), 4727-4745. doi:https://doi.org/10.1029/2018JD028290

Lindaas, J., Pollack, I. B., Garofalo, L. A., Pothier, M. A., Farmer, D. K., Kreidenweis, S. M., Campos, T. L., Flocke, F., Weinheimer, A. J., Montzka, D. D., Tyndall, G. S., Palm, B. B., Peng, Q., Thornton, J. A., Permar, W., Wielgasz, C., Hu, L., Ottmar, R. D., Restaino, J. C., Hudak, A. T., Ku, I-T., Zhou, Y., Sive, B. C., Sullivan, A., Collett Jr, J. L.,
350 Fischer, E. V. (2021). Emissions of Reactive Nitrogen From Western U.S. Wildfires During Summer 2018. *Journal of Geophysical Research: Atmospheres, 126*(2), e2020JD032657. doi:https://doi.org/10.1029/2020JD032657

Liu, X., Huey, L. G., Yokelson, R. J., Selimovic, V., Simpson, I. J., Müller, M., , & Jimenez, J. L., Campuzano-Jost, P., Beyersdorf, A. J., Blake, D. R., Butterfield, Z., Choi, Y., Crounse, J. D., Day, D. A., Diskin, G. S., Dubey, M. K., Fortner, E., Hanisco, T. F., Hu, W., King, L. E., Kleinman, L., Meinardi, S., Mikoviny, T., Onasch, T. B., Palm, B. B., Peischl, J., Pollack, I. B., Ryerson, T. B., Sachse, G. W., Sedlacek, A. J., Shilling, J. E., Springston, S., St. Clair, J. M., Tanner, D. J., Teng, A. P., Wennberg, P. O., Wisthaler, A., Wolfe, G. M. (2017). Airborne measurements of western U.S. wildfire emissions: Comparison with prescribed burning and air quality implications. *Journal of Geophysical Research: Atmospheres, 122*(11), 6108-6129. doi:10.1002/2016jd026315

Lobert, J. M., Scharffe, D. H., Hao, W. M., & Crutzen, P. J. (1990). Importance of biomass burning in the atmospheric budgets of nitrogen-containing gases. *Nature, 346*(6284), 552-554. doi:10.1038/346552a0

McMeeking, G. R., Kreidenweis, S. M., Baker, S., Carrico, C. M., Chow, J. C., Collett, J. L., Hao, W. M., Holden, A. S., Kirchstetter, T. W., Malm, W. C., Moosmüller, H., Sullivan, A. P., Wold, C. E. (2009). Emissions of trace gases and aerosols during the open combustion of biomass in the laboratory. *Journal of Geophysical Research, 114*(D19). doi:10.1029/2009jd011836

Müller, M., Mikoviny, T., Feil, S., Haidacher, S., Hanel, G., Hartungen, E., Jordan, A., Märk, L., Mutschlechner, P., Schottkowsky, R. (2014). A compact PTR-ToF-MS instrument for airborne measurements of volatile organic compounds at high spatiotemporal resolution. *Atmos. Meas. Tech., 7*(11), 3763-3772. doi:10.5194/amt-7-3763-2014

Müller, M., Mikoviny, T., Feil, S., Haidacher, S., Hanel, G., Hartungen, E., Jordan, A., Märk, L., Mutschlechner, P., Schottkowsky, R., Anderson, B. E., Beyersdorf, A. J., Crawford, J. H., Diskin, G. S., Eichler, P., Fried, A., Keutsch, F. N., Mikoviny, T., Thornhill, K. L., Walega, J. G., Weinheimer, A. J., Yang, M., Yokelson, R. J., Wisthaler, A. (2016). In situ measurements and modeling of reactive trace gases in a small biomass burning plume. *Atmos. Chem. Phys., 16*(6), 3813-3824. doi:10.5194/acp-16-3813-2016

Müller, M., Piel, F., Gutmann, R., Sulzer, P., Hartungen, E., Wisthaler, A. (2020). A novel method for producing NH4+ reagent ions in the hollow cathode glow discharge ion source of PTR-MS instruments. *International Journal of Mass Spectrometry, 447*, 116254. doi:10.1016/j.ijms.2019.116254

NASA, Fire Influence on Regional to Global Environments and Air Quality, NASA Earthdata, doi: 10.5067/SUBORBITAL/FIREXAQ2019/DATA001, 2019.

Nault, B. A., Campuzano-Jost, P., Day, D. A., Jo, D. S., Schroder, J. C., Allen, H. M., Bahreini, R., Bian, H., Blake, D. R., Chin, M., Clegg, S. L., Colarco, P. R., Crounse, J. D., Cubison, M. J., DeCarlo, P. F., Dibb, J. E., Diskin, G. S., Hodzic, A., Hu, W., Katich, J. M., Kim, M. J., Kodros, J. K., Kupc, A., Lopez-Hilfiker, F. D., Marais, E. A., Middlebrook, A. M., Neuman, A. J., Nowak, J. B., Palm, B. B., Paulot, F., Pierce, J. R., Schill, G. P., Scheuer, E., Thornton, J. A., Tsigaridis, K., Wennberg, P. O., Williamson, C. J., Jimenez, Jose L. (2021). Chemical transport models often underestimate inorganic aerosol acidity in remote regions of the atmosphere. *Communications Earth & Environment, 2*(1), 93. doi:10.1038/s43247-021-00164-0

Ottmar, R. D., Sandberg, D.V., Riccardi, C. L., Prichard, S.J. (2007). An overview of the Fuel Characteristic Classification System — Quantifying, classifying, and creating fuelbeds for resource planning. *Canadian Journal of Forest Research, 37*(12), 2383-2393. doi:10.1139/x07-077

Pan, D., Benedict, K. B., Golston, L. M., Wang, R., Collett, J. L., Tao, L., Sun, K., Guo, X., Ham, J., Prenni, A. J., Schichtel, B. A., Mikoviny, T., Müller, M., Wisthaler, A., Zondlo, M. A. (2021). Ammonia Dry Deposition in an Alpine Ecosystem Traced to Agricultural Emission Hotpots. *Environmental Science & Technology, 55*(12), 7776-7785. doi:10.1021/acs.est.0c05749

Piel, F., Müller, M., Winkler, K., Skytte af Sätra, J., & Wisthaler, A. (2021). Introducing the extended volatility range proton-transfer-reaction mass spectrometer (EVR PTR-MS). *Atmos. Meas. Tech., 14*(2), 1355-1363. doi:10.5194/amt-14-1355-2021

Prichard, S. J., O'Neill, S. M., Eagle, P., Andreu, A. G., Drye, B., Dubowy, J., Urbanski, S., Strand, T. M. (2020). Wildland fire emission factors in North America: synthesis of existing data, measurement needs and management applications. *International Journal of Wildland Fire, 29*(2), 132-147. doi:https://doi.org/10.1071/WF19066

Pye, H. O. T., Nenes, A., Alexander, B., Ault, A. P., Barth, M. C., Clegg, S. L., Collett Jr, J. L., Fahey, K. M., Hennigan, C. J., Herrmann, H., Kanakidou, M., Kelly, J. T., Ku, I. T., McNeill, V. F., Riemer, N., Schaefer, T., Shi, G., Tilgner, A., Walker, J. T., Wang, T., Weber, R., Xing, J., Zaveri, R. A., Zuend, A. (2020). The acidity of atmospheric particles and clouds. *Atmos. Chem. Phys., 20*(8), 4809-4888. doi:10.5194/acp-20-4809-2020

Roberts, J. M., Stockwell, C. E., Yokelson, R. J., de Gouw, J., Liu, Y., Selimovic, V., Koss, A. R., Sekimoto, K., Coggon, M. M., Yuan, B., Zarzana, K. J., Brown, S. S., Santin, C., Doerr, S. H., Warneke, C. (2020). The nitrogen budget of laboratory-simulated western US wildfires during the FIREX 2016 Fire Lab study. *Atmos. Chem. Phys., 20*(14), 8807-8826. doi:10.5194/acp-20-8807-2020

Sachse, G., Collins, J., Hill, G., Wade, L., Burney, L., Ritter, J. (1991). Airborne tunable diode laser sensor for high-precision concentration and flux measurements of carbon monoxide and methane. In *Measurement of atmospheric gases* (Vol. 1433). Los Angeles, CA, United States: Proc. SPIE.

Seinfeld, J. H., Pandis, S. N. (2016). *Atmospheric Chemistry and Physics: From Air Pollution to Climate Change*: John Wiley & Sons.

Selimovic, V., Yokelson, R. J., Warneke, C., Roberts, J. M., de Gouw, J., Reardon, J., Griffith, D. W. T. (2018). Aerosol optical properties and trace gas emissions by PAX and OP-FTIR for laboratory-simulated western US wildfires during FIREX. *Atmos. Chem. Phys., 18*(4), 2929-2948. doi:10.5194/acp-18-2929-2018

Stockwell, C. E., Veres, P. R., Williams, J., & Yokelson, R. J. (2015). Characterization of biomass burning emissions from cooking fires, peat, crop residue, and other fuels with high-resolution proton-transfer-reaction time-of-flight mass spectrometry. *Atmos. Chem. Phys., 15*(2), 845-865. doi:10.5194/acp-15-845-2015

Sun, K., Cady-Pereira, K., Miller, D. J., Tao, L., Zondlo, M. A., Nowak, J. B., Neuman, J. A., Mikoviny, T., Müller, M., Wisthaler, A., Scarino, A. J., Hostetler, C. A. (2015). Validation of TES ammonia observations at the single pixel scale in the San Joaquin Valley during DISCOVER-AQ. *Journal of Geophysical Research: Atmospheres, 120*(10), 5140-5154. doi:https://doi.org/10.1002/2014JD022846

Vay, S. A., Tyler, S. C., Choi, Y., Blake, D. R., Blake, N. J., Sachse, G. W., Diskin, G. S., Singh, H. B. (2009). Sources and transport of Delta14C in CO2 within the Mexico City Basin and vicinity. *Atmos. Chem. Phys., 9*(14), 4973-4985. doi:10.5194/acp-9-4973-2009

Warneke, C., J.P. Schwarz, J.E. Dibb, O. Kalashnikova, G. Frost, J. Al-Saadi, S.S. Brown, W.A. Brewer, A. Soja, F.C. Seidel, R.A. Washenfelder, E.B. Wiggins, R.H. Moore, B.E. Anderson, C. Jordan, T.I. Yacovitch, S.C. Herndon, S. Liu, T. Kuwayama, D. Jaffe, N. Johnston, V. Selimovic, R. Yokelson, D.M. Giles, B.N. Holben, P. Goloub, I. Popovici, M. Trainer, Ad. Kumar, R.B. Pierce, D. Fahey, J. Roberts, E.M. Gargulinski, D.A. Peterson, X. Ye, L.H. Thapa, P.E. Saide, C.H. Fite, C.D. Holmes, S. Wang, M.M. Coggon, Z.C.J. Decker, C.E. Stockwell, L. Xu, G. Gkatzelis, K. Aikin, B. Lefer, J. Kaspari, D. Griffin, L. Zeng, R. Weber, M. Hastings, J. Chai, G.M. Wolfe, T.F. Hanisco, J. Liao, P. Campuzano-Jost, H. Guo, J.L. Jimenez, J. Crawford, And The FIREX-AQ science team. (2022). Fire Influence on Regional to Global Environments and Air Quality (FIREX-AQ) *Journal of Geophysical Research, Submitted Aug. 2022*.

Yokelson, R. J., Burling, I. R., Gilman, J. B., Warneke, C., Stockwell, C. E., de Gouw, J., Akagi, S. K., Urbanski, S. P., Veres, P., Roberts, J. M., Kuster, W. C., Reardon, J., Griffith, D. W. T., Johnson, T. J., Hosseini, S., Miller, J. W., Cocker Iii, D. R., Jung, H., Weise, D. R. (2013). Coupling field and laboratory measurements to estimate the emission factors of identified and unidentified trace gases for prescribed fires. *Atmos. Chem. Phys., 13*(1), 89-116. doi:10.5194/acp-13-89-2013

Yokelson, R. J., Goode, J. G., Ward, D. E., Susott, R. A., Babbitt, R. E., Wade, D. D., Bertschi, I., Griffith, D. W. T., Hao, W. M. (1999). Emissions of formaldehyde, acetic acid, methanol, and other trace gases from biomass fires in North Carolina measured by airborne Fourier transform infrared spectroscopy. *Journal of Geophysical Research: Atmospheres, 104*(D23), 30109-30125. doi:https://doi.org/10.1029/1999JD900817

Yokelson, R. J., Griffith, D. W. T., Ward, D. E. (1996). Open-path Fourier transform infrared studies of large-scale laboratory biomass fires. *Journal of Geophysical Research: Atmospheres, 101*(D15), 21067-21080. doi:https://doi.org/10.1029/96JD01800

Yokelson, R. J., Susott, R., Ward, D. E., Reardon, J., Griffith, D. W. T. (1997). Emissions from smoldering combustion of biomass measured by open-path Fourier transform infrared spectroscopy. *Journal of Geophysical Research: Atmospheres, 102*(D15), 18865-18877. doi:https://doi.org/10.1029/97JD00852